Journal of Engineering and Science Research 7 (3): 26-31, 2023
e-ISSN: 2289-7127

DOI: 10.26666/rmp.jesr.2023.3.4

Adaptive Wavelet De-noising Algorithm using Absolute Difference Optimization Technique for Partial Discharge Signal

Chin Kui Fern[1], Chai Chang Yii[2,*], Asfarina Abu Bakar[1], Ismail Saad[2],Herwansyah Lago[2], Pungut Ibrahim[2], Ahmad Razani Haron[2]

[1]Faculty of Science & Technology, i-CATS University College, Kuching, Sarawak, Malaysia.
[2]School of Electrical Electronics Engineering, Faculty of Engineering, Universiti Malaysia Sabah, Kota Kinabalu, Sabah, Malaysia.
*Corresponding Author: chaichangyii@ums.edu.my

Received: 30 March 2023; Revised: 15 April 2023; Accepted: 01 May 2023; Published: 30 June 2023

Abstract: Discrete Wavelet Transform (DWT) de-noising method is widely used for one-dimension partial discharge (PD) signals measured from medium voltage underground cable. However, DWT de-noising has several drawbacks that prevent the DWT de-noising from improving its de-noising effectiveness In DWT de-noising, the two most important parameters are decomposition level and mother wavelet. The aforementioned parameters must be varied according to the noise level in the measured PD signal in order to effectively suppress the noise of the measured PD signal. In this paper, an adaptive DWT de-noising algorithm based on the Absolute Difference Optimizing (ADO) technique is presented to effectively suppress the varying noise levels in measured PD signal. First, the measured PD signal will be de-noised using a Daubechies 3 (db3) mother wavelet and a DWT decomposition level ranging from 1 to 10. Second, the de-noised PD signal will be subjected to the ADO technique. The sum of the absolute difference of local maxima in the de-noised PD signal will be used as an indicator to select the best decomposition level for the de-noised PD signal. Finally, the best-selected de-noised PD signal by using the ADO technique will be used to estimate the PD location on the underground cable. The results of PD location error using the ADO technique and normal DWT de-noising will be compared. The findings show that the ADO-based adaptive DWT de-noising algorithm significantly improved the de-noising process of the measured PD signal.

.

Keywords: DWT, Partial Discharge, Absolute Difference Optimization

1. Introduction

Partial discharge (PD) in underground cables is a localized short-duration electrical pulse caused by an accumulation of electrical stress in the insulation system or on the insulation's surface [1]. Early detection of insulation defects is critical because PD can cause damage to underground cables. Extensive research on the phenomenon of PD that has been carried out includes feature extraction techniques [2-5], defect location and identification techniques [6,7], physical and chemical processes [8,9], denoising techniques [10-15], and pulse classification techniques [16-19].

There are numerous types of PD measurements available in the market, including optical, acoustic, electrical, and chemical byproduct analysis [20-24]. PD sensors such as High-Frequency Current Transformer (HCFT) and Ultra High Frequency (UHF), detect not only high-frequency signals starting at Mega Hertz (MHz) but also unwanted signals such as noise. The presence of noise and interference reduces measurement sensitivity especially when low-energy online PD pulses are present. Another drawback of online PD measurement occurs when the test detects multiple pulse signal sources.

PD denoising is a salient task in online PD monitoring systems. To accurately de-noise PD signals, advanced methods such as Artificial Neural Networks (ANN) [13,14] and deep learning [25,26] are required. Wavelet transform-based methods for PD denoising white noise have been reported in several studies [27-29]. The wavelet transform signal, on the other hand, is closely related to the selected mother wavelet and the level of decomposition [30].

Corresponding Author: Chai Chang Yii, School of Electrical Electronics Engineering, Faculty of Engineering, Universiti Malaysia Sabah, Kota Kinabalu, Sabah, Malaysia.. Email: chaichangyii@ums.edu.my

The standard DWT de-noising technique for a one-dimension PD signal must set a fixed decomposition level to suppress the noise detected by the PD sensor. However, due to differences in environmental noise levels, the noise detected by the sensor is not effectively suppressed by standard DWT denoising techniques. Thus, an adaptive DWT De-noising Algorithm that implements the Absolute Difference Optimization (ADO) technique is introduced in this paper to automatically select the best decomposition level to suppress the noise without eliminating its PD signal.

2. Adaptive Wavelet De-noising

. In this research work, the adaptive wavelet de-noising algorithm will be divided into three phases: modeling of the input signal, development of a new method of adaptive wavelet de-noising using the ADO technique, and finally application of the PD location algorithm to validate the effectiveness of de-noising by comparing the error of estimated PD location. The method of input signal modeling, which includes PD signal modeling and noise modeling will be explained in sub-section 2.1. The method of the ADO technique in selecting the decomposition level of DWT de-noising will be explained in sub-section 2.2. Finally, the PD location algorithm used in estimating PD location will be explained in sub-section 2.3.

2.1. PD Signal and Environmental Noise Modeling

In the MATLAB environment simulation, the PD pulse mathematical model and PD propagation velocity along the underground cable must be determined. A mathematical model, as shown in Equation 1 [31], can be used to simulate the onsite measured PD signal from a PD sensor.

$$s(t) = A[e^{-a_1 t}\cos(w_d t - \varphi) - e^{-a_2 t}\cos(\varphi)] \quad (1)$$

where A is the magnitude coefficient assumed to be 0.01, $a_1 = 1\ \mathrm{Ms}^{-1}$, $a_2 = 10\ \mathrm{Ms}^{-1}$, $\varphi = \tan^{-1}\left({}^{w_d}/_{a_2}\right)$, $w_d = 2\pi f_d$, and $f_d = 1$ MHz. The simulative sampling frequency, f_s is 100 MHz.

In addition, the propagation velocity of the three cores $50\ mm^2\ Cu/XLPE/PVC, 8.7/15\ kV$ underground cable is $156\ m/\mu s$ as reported in [32]. The time delay in simulating the PD signal will be computed using the propagation velocity of the PD signal travelling along the cable. Furthermore, using the MATLAB function "awgn," 5 levels of white Gaussian noise (WGN) will be added to the simulated PD signal. The WGN noise level will be decremented in 5 dB steps from 5 dB to -20 dB signal to noise ratio (SNR). The results of the simulated PD signal with WGN are shown in sub-section 3.1.

2.2. Absolute Difference Optimization Technique

The adaptive wavelet de-noising algorithm will use the modeled PD signals along with varying levels of WGN. The adaptive wavelet de-noising algorithm's entire process flow is depicted in Figure 1. The algorithm begins by incorporating modeled PD signals with varying noise levels. Next, each of the noise-affected modeled PD signals will be de-noised using DWT with a fixed "Daubechies 3" (db3) mother wavelet and varying decomposition levels. The DWT de-noising decomposition levels are varied from 1 to 10 with a 1-level step increment. The de-noised PD signals will then be absolute as a pre-processing step before applying the ADO technique. The ADO technique is composed of two steps: computing the absolute difference (AD) of de-noised PD signals using the MATLAB function "findpeaks" and computing the ADO factor using Equation 2.

$$ADO = \sum AD - K \quad (2)$$

where, $\sum AD$ is the summation of total local maxima in the PD signal and K is the constant optimization value for DWT de-noising by using db3 mother wavelet.

The lower the value of the ADO factor, the more efficient the PD signal de-noising process. The ADO technique can thus determine the best decomposition level of DWT de-noising for each noise level. Finally, the best de-noised PD signals will be chosen and used to estimate PD location on underground cables.

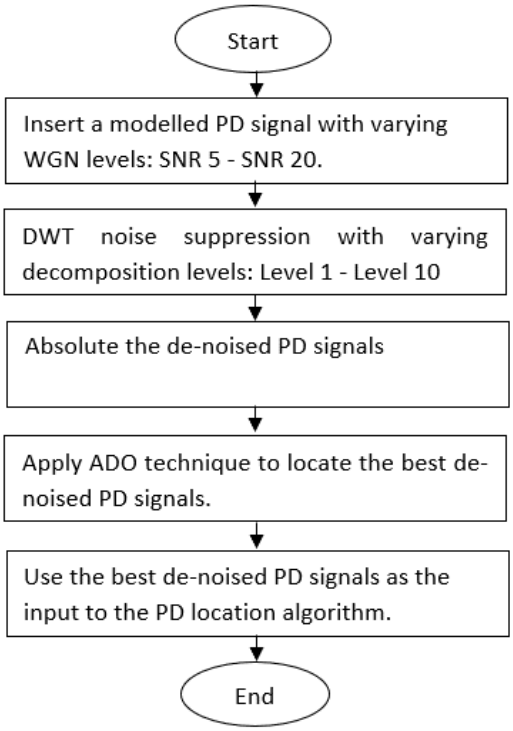

Figure 1. Flow chart of adaptive wavelet de-noising

2.3. Estimated PD Location

The simulation model of on-line PD location estimation system for underground ground cable in this research is

based on double-end PD location algorithm. Figure 2 shows an online PD location estimation system for underground cables. In this model, double-end PD location measuring method will be used. Two PD sensors, PD sensor A and PD sensor B, are clamped at the underground cable's front and tail ends. The PD sensors are spaced 2 kilometers apart. PD occurs at 1.3 km from the front end of the underground cable. The measured PD signals from PD sensors A and B will be sent to the substation control panel for PD location estimation using the PD location algorithm. The PD location algorithm will be fed the best de-noised PD signal from adaptive wavelet de-noising.

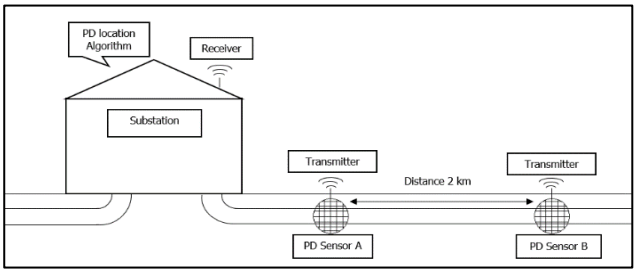

Figure 2. Online PD location estimation system for underground cables

The cross-correlation technique will be used to find the strongest bonding between the two de-noised PD signals from PD sensor A and PD sensor B. The cross-correlation factor mathematical equation is as follows:

$$CCF_{AB} = \sum_{n=0}^{10000} A[n] \times B[n] \quad (3)$$

where, $A[n]$ is the de-noised PD signal from PD sensor A and $B[n]$ is the de-noised PD signal from PD sensor B. According to Equation (3), the cross-correlation factor for $Signal\ A[n]$ and $Signal\ B[n]$ (CCF_{AB}) is computed by shifting $Signal\ A[n]$ by one sample to the right, then multiplying $Signal\ A[n]$ with $Signal\ B[n]$, and finally summing the product of $Signal\ A[n]$ and $Signal\ B[n]$. This process of shifting, multiplying and summing is repeated ten thousand times until the adjacent signal is shifted one full cycle. The CCF_{AB} will be converted into time different, T_{AB} and the estimated PD location can be obtained using Equation (4).

$$PD\ location = 0.5(L - v * T_{AB}) \quad (4)$$

where, L is the total monitored cable length, v is the propagation velocity of PD signal along the cable, and T_{AB} is the time different between $Signal\ A[n]$ and $Signal\ B[n]$

3. Result and Discussion

The results of the adaptive wavelet de-noising algorithm can be divided into three sections. Sub-section 3.1 shows the results of the simulated PD signal and DWT de-noising, sub-section 3.2 shows the results and analysis of DWT de-noising performance by using ADO technique, and sub-section 3.3 shows the effect of ADO technique on reducing the percentage error of the estimated PD location.

3.1. Simulated PD Signal and Wavelet De-noising

In sub-section 2.3, the simulation model of an online PD location estimation system for underground cable will generate two measuring PD signals from PD Sensor A and PD Sensor B. Equation 1 is used to calculate the generated PD signals, which consider the PD signal propagation velocity in the underground cable. Figure 3 (a) and Figure 3 (b) show simulated $Signal\ A[n]$ from PD Sensor A and simulated $Signal\ B[n]$ from PD Sensor B with minimum noise of 5 dB SNR. Figure 4 (a) and Figure 4 (b) depict simulated $Signal\ A[n]$ from PD Sensor A and simulated $Signal\ B[n]$ from PD Sensor B with maximum noise of -20 dB SNR. When comparing Figures 3 and 4, the PD pulse in Figure 3 can still be seen, whereas the PD pulse in Figure 4 is submerged in the WGN. As a result, before incorporating the PD location algorithm, the measured PD signal must be de-noised.

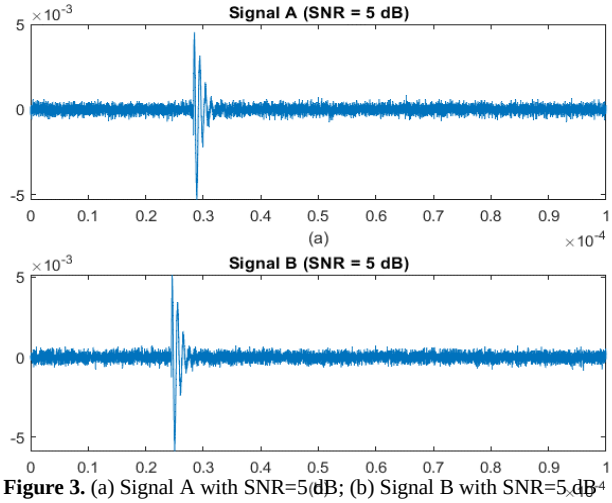

Figure 3. (a) Signal A with SNR=5 dB; (b) Signal B with SNR=5 dB

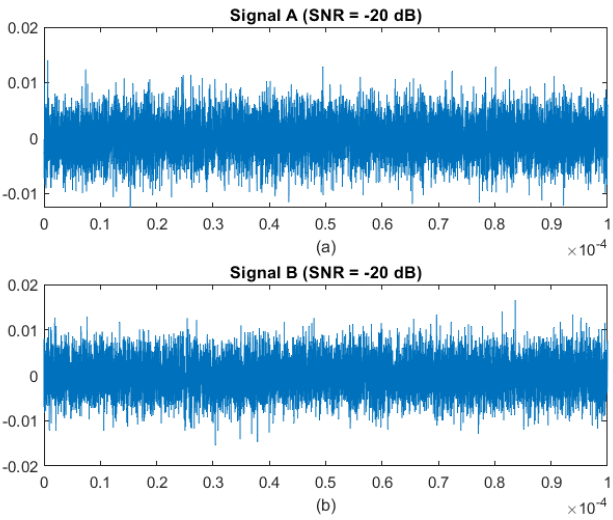

Figure 4. (a) Signal A with SNR=-20 dB; (b) Signal B with SNR=-20 dB

In this paper, DWT de-noising with decomposition levels ranging from 1 to 10 is applied to a simulated PD signal with SNR ranging from 5 to -20dB. Figure 5 shows the results of DWT de-nosing on simulated $Signal\ A[n]$ with -20 dB SNR using decomposition levels 1, 5, and 10. The DWT de-noising with decomposition level 1 is insufficient, according to the comparison of decomposition levels in sub-figures 5(a), 5(b), and 5(c), because the de-noised signal still contains a significant amount of noise. Meanwhile, the DWT de-noising with decomposition level 10 outperforms because the PD pulse has been eliminated from the de-noised signal. The DWT de-noising with decomposition level 5 performs the best of the three de-noised signals because it remains the PD pulse while suppressing a large amount of noise. Thus, selecting the appropriate decomposition level for a specific noise level is critical for effective PD signal de-noising.

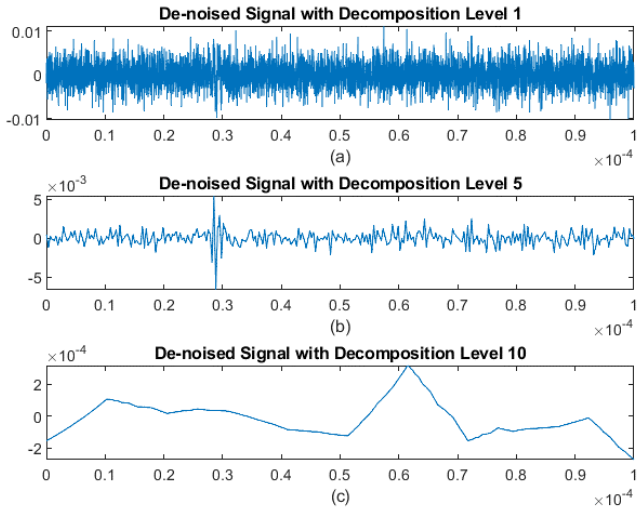

Figure 5. (a) De-noised signal with decomposition level 1; (b) De-noised signal with decomposition level 5; (c) De-noised signal with decomposition level 10

3.2. Adaptive Wavelet De-noising with ADO technique

ADO is a novel method for determining the best decomposition level for DWT de-noising in relation to the noise level. Table 1 displays the results of DWT de-noising on PD signals with an SNR of 5dB. With the condition that db3 is used as the mother wavelet, the lowest ADO factor indicates the best decomposition level for DWT de-noising. As a result, decomposition level 1 is the best choice for DWT de-noising on PD signals with 5 dB SNR because the lowest ADO factor (0.0829) yields the lowest PD location error (0.0173%).

Table 1. ADO factor for PD signal with 5 dB SNR

SNR	AD	ADO	Estimated PD location (m)	PD Location Error (%)	Decomposition Level (DWT)
5	0.3171	0.0829	1299.65	0.0173	1
5	0.1670	0.2330	1299.65	0.0173	2
5	0.0930	0.3070	1299.65	0.0173	3
5	0.0470	0.3530	1299.65	0.0173	4
5	0.0336	0.3664	1299.65	0.0173	5
5	0.0126	0.3874	1299.65	0.0173	6
5	0.0029	0.3971	1298.09	0.0953	7
5	0.0012	0.3988	2598.94	64.9469	8
5	0.0004	0.3996	2166.62	43.3312	9
5	0.0001	0.3999	1115.49	9.2254	10

Table 2 shows the result of DWT de-noising on PD signals with -10 dB SNR. The decomposition level 3 is the most suitable decomposition level for DWT de-noising on PD signals with 5 dB SNR because the lowest ADO factor (0.0575) yields the lowest PD location error (0.0173 %). Table 3 shows the result of DWT de-noising on PD signals with an SNR of -20dB. The decomposition level 4 is the best decomposition level for DWT de-noising on PD signals with 5 dB SNR because the lowest ADO factor (0.5591) yields the lowest PD location error (0.0173 %). Based on Table 1, Table 2, and Table 3, the AD value closest to 0.4 shows the best decomposition level. Thus K=0.4 is selected as the constant optimization value for DWT de-noising by using the db3 mother wavelet in Equation 2.

Table 2. ADO factor for PD signal with -10 dB SNR

SNR	AD	ADO	Estimated PD location (m)	PD Location Error (%)	Decomposition Level (DWT)
-10	1.6081	1.2081	1302.78	0.1388	1
-10	0.8630	0.4630	1302.78	0.1388	2
-10	0.4575	0.0575	1299.65	0.0173	3
-10	0.1739	0.2261	1299.65	0.0173	4
-10	0.0859	0.3141	1299.65	0.0173	5
-10	0.0329	0.3671	1299.65	0.0173	6
-10	0.0105	0.3895	2602.06	65.1029	7
-10	0.0034	0.3966	1803.76	25.1880	8
-10	0.0021	0.3979	1726.51	21.3253	9
-10	0.0011	0.3989	1787.37	24.3687	10

Table 3. ADO factor for PD signal with -20 dB SNR

SNR	AD	ADO	Estimated PD location (m)	PD Location Error (%)	Decomposition Level (DWT)
-20	5.0767	4.6767	4363.31	153.1654	1
-20	2.6632	2.2632	1293.41	0.3294	2
-20	1.4728	1.0728	1343.35	2.1677	3
-20	0.5591	0.1591	1299.65	0.0173	4
-20	0.2353	0.1647	1300.43	0.0217	5
-20	0.0961	0.3039	1298.87	0.0563	6
-20	0.0368	0.3632	1600.09	15.0045	7
-20	0.0169	0.3831	4399.20	154.9602	8
-20	0.0070	0.3930	1067.89	11.6055	9
-20	0.0029	0.3971	1189.63	5.5187	10

Table 4 displays the best decomposition level of DWT de-noising in terms of the lowest ADO factor for a noise-corrupted signal with SNR ranging from 5 dB to -20 dB and a 5dB step decrement. According to Table 4, the higher the noise level or the lower the SNR, the higher the decomposition level for DWT de-noising is required to efficiently suppress the noise without eliminating the PD pulse. The graph in Figure 6 depicts the estimated PD location error versus decomposition level. According to the graph in Figure 6, any decomposition level higher than level 6 will result in inefficient DWT de-noising, resulting in a high estimated PD location error. Decomposition levels 1, 2, and 3 will also result in inefficient DWT de-noising for signals with -20 dB SNR.

.

Table 4. The best decomposition level of DWT de-noising for various noise level

SNR	AD	ADO	Estimated PD location (m)	PD Location Error (%)	Decomposition Level (DWT)
5	0.3171	0.0829	1299.65	0.0173	1
0	0.2877	0.1123	1299.65	0.0173	2
-5	0.4939	0.0939	1299.65	0.0173	2
-10	0.4575	0.0575	1299.65	0.0173	3
-15	0.3292	0.0708	1299.65	0.0173	4
-20	0.5591	0.1591	1299.65	0.0173	4

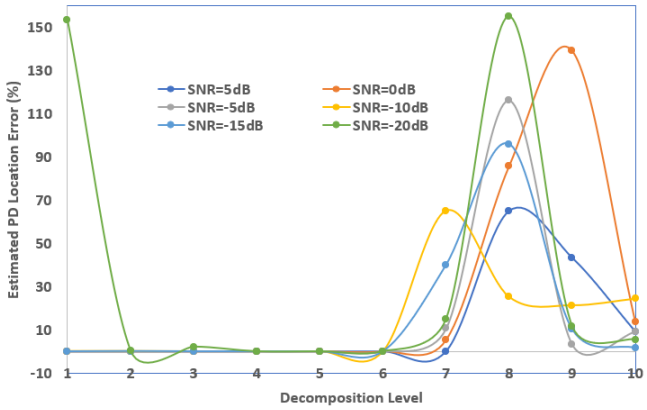

Figure 5. Graph of estimated PD location error versus decomposition level

4. Conclusion

The adaptive wavelet de-noising algorithm based on the ADO technique has been shown to improve the performance of DWT by automatically selecting the best decomposition level based on the noise in the PD signal. The findings show that the higher the noise level in PD signal, the higher the decomposition level required for effective DWT de-noising. The adaptive wavelet de-noising algorithm can be improved in the future by automating the selection of the mother wavelet for DWT de-noising.

Acknowledgements

This research was funded by a grant from Universiti Malaysia Sabah. (SPLB Grant: SLB2204). The authors would like to thank High Voltage Laboratory and HiPER UMS for their technical support.

REFERENCES

[1] IEC, IEC 60270 High-voltage test techniques: Partial discharge measurements, 2000.

[2] Li, Ze, et al. “Partial Discharge Fault Diagnosis Based on Zernike Moment and Improved Bacterial Foraging Optimization Algorithm.” *Electric Power Systems Research*, vol. 207, June 2022, p. 107854. *DOI.org (Crossref)*, https://doi.org/10.1016/j.epsr.2022.107854.

[3] Soh, Donny, et al. “Partial Discharge Diagnostics: Data Cleaning and Feature Extraction.” *Energies*, vol. 15, no. 2, Jan. 2022, p. 508. *DOI.org (Crossref)*, https://doi.org/10.3390/en15020508.

[4] Florkowski, Marek. “Anomaly Detection, Trend Evolution, and Feature Extraction in Partial Discharge Patterns.” *Energies*, vol. 14, no. 13, June 2021, p. 3886. *DOI.org (Crossref)*, https://doi.org/10.3390/en14133886.

[5] Hassan, Waqar, et al. “Feature Extraction of Partial Discharges During Multiple Simultaneous Defects in Low-Voltage Electric Machines.” *IEEE Transactions on Instrumentation and Measurement*, vol. 70, 2021, pp. 1–10. *DOI.org (Crossref)*, https://doi.org/10.1109/TIM.2021.3101301

[6] Gulski, Edward, et al. “On-Site Testing and PD Diagnosis of High Voltage Power Cables.” *IEEE Transactions on Dielectrics and Electrical Insulation*, vol. 15, no. 6, Dec. 2008, pp. 1691–700. *DOI.org (Crossref)*, https://doi.org/10.1109/TDEI.2008.4712673.

[7] Kreuger, F. H., et al. “Classification of Partial Discharges.” *IEEE Transactions on Electrical Insulation*, vol. 28, no. 6, Dec. 1993, pp. 917–31. *DOI.org (Crossref)*, https://doi.org/10.1109/14.249365.

[8] Borsi, H. “Study about the Physical Processes Leading to Partial Discharges in Insulating Fluids.” *European Transactions on Electrical Power*, vol. 9, no. 6, Nov. 1999, pp. 363–67. *DOI.org (Crossref)*, https://doi.org/10.1002/etep.4450090603.

[9] Van Brunt, R. J. “Physics and Chemistry of Partial Discharge and Corona. Recent Advances and Future Challenges.” *IEEE Transactions on Dielectrics and Electrical Insulation*, vol. 1, no. 5, Oct. 1994, pp. 761–84. *DOI.org (Crossref)*, https://doi.org/10.1109/94.326651.

[10] Li, Shanjun, et al. “Partial Discharge Signal Denoising Method Based on Frequency Spectrum Clustering and Local Mean Decomposition.” *IET Science, Measurement & Technology*, vol. 14, no. 10, Dec. 2020, pp. 853–61. *DOI.org (Crossref)*, https://doi.org/10.1049/iet-smt.2020.0061.

[11] Dhandapani, Ragavesh, et al. “Enhanced Partial Discharge Signal Denoising Using Dispersion Entropy Optimized Variational Mode Decomposition.” *Entropy*, vol. 23, no. 12, Nov. 2021, p. 1567. *DOI.org (Crossref)*, https://doi.org/10.3390/e23121567,

[12] Zaeni, A., et al. "Partial Discharge Signal Denoising by Using Hard Threshold and Soft Threshold Methods and Wavelet Transformation." *IOP Conference Series: Materials Science and Engineering*, vol. 602, no. 1, Aug. 2019, p. 012034. *DOI.org (Crossref)*, https://doi.org/10.1088/1757-899X/602/1/012034

[13] Soltani, Amir Abbas, and Ayman El-Hag. "Denoising of Radio Frequency Partial Discharge Signals Using Artificial Neural Network." *Energies*, vol. 12, no. 18, Sept. 2019, p. 3485. *DOI.org (Crossref)*, https://doi.org/10.3390/en12183485.

[14] N. A. Yusoff *et al*., "Denoising technique for partial discharge signal : A comparison performance between artificial neural network, fast fourier transform and discrete wavelet transform," *2016 IEEE International Conference on Power and Energy (PECon)*, 2016, pp. 311-316, doi: 10.1109/PECON.2016.7951579.

[15] Sriram, S., et al. "Signal Denoising Techniques for Partial Discharge Measurements." *IEEE Transactions on Dielectrics and Electrical Insulation*, Dec. 2005, pp. 1182–91. *DOI.org (Crossref)*, https://doi.org/10.1109/TDEI.2005.1561798.

[16] Hui Ma, et al. "Pattern Recognition Techniques and Their Applications for Automatic Classification of Artificial Partial Discharge Sources." *IEEE Transactions on Dielectrics and Electrical Insulation*, vol. 20, no. 2, Apr. 2013, pp. 468–78. *DOI.org (Crossref)*, https://doi.org/10.1109/TDEI.2013.6508749

[17] Ardila-Rey, J., et al. "Partial Discharge and Noise Separation by Means of Spectral-Power Clustering Techniques." *IEEE Transactions on Dielectrics and Electrical Insulation*, vol. 20, no. 4, Aug. 2013, pp. 1436–43. *DOI.org (Crossref)*, https://doi.org/10.1109/TDEI.2013.6571466

[18] Ardila-Rey, Jorge, et al. "Inductive Sensor Performance in Partial Discharges and Noise Separation by Means of Spectral Power Ratios." *Sensors*, vol. 14, no. 2, Feb. 2014, pp. 3408–27. *DOI.org (Crossref)*, https://doi.org/10.3390/s140203408.

[19] Cavallini, A., et al. "A New Approach to the Diagnosis of Solid Insulation Systems Based on PD Signal Inference." *IEEE Electrical Insulation Magazine*, vol. 19, no. 2, Mar. 2003, pp. 23–30. *DOI.org (Crossref)*, https://doi.org/10.1109/MEI.2003.1192033.

[20] Wang, Lutang, et al. "A Fiber Optic PD Sensor Using a Balanced Sagnac Interferometer and an EDFA-Based DOP Tunable Fiber Ring Laser." *Sensors*, vol. 14, no. 5, May 2014, pp. 8398–422. *DOI.org (Crossref)*, https://doi.org/10.3390/s140508398.

[21] Posada-Roman, Julio, et al. "Fiber Optic Sensor for Acoustic Detection of Partial Discharges in Oil-Paper Insulated Electrical Systems." *Sensors*, vol. 12, no. 4, Apr. 2012, pp. 4793–802. *DOI.org (Crossref)*, https://doi.org/10.3390/s120404793.

[22] Haddad, A.; Warne, D.F. *Advances in High Voltage Engineering*, 2nd ed.; IET Power and Energy Series; IET: London, UK, 2007; pp. 37–190. [Google Scholar]

[23] Wang, X., et al. "Acousto-Optical PD Detection for Transformers." *IEEE Transactions on Power Delivery*, vol. 21, no. 3, July 2006, pp. 1068–73. *DOI.org (Crossref)*, https://doi.org/10.1109/TPWRD.2005.861242.

[24] Tian, Y., et al. "Comparison of On-Line Partial Discharge Detection Methods for HV Cable Joints." *IEEE Transactions on Dielectrics and Electrical Insulation*, vol. 9, no. 4, Aug. 2002, pp. 604–15. *DOI.org (Crossref)*, https://doi.org/10.1109/TDEI.2002.1024439.

[25] Sukumar, T., et al. "Recognition of Single and Multiple Partial Discharge Patterns Using Deep Learning Algorithm." *2021 International Conference on Artificial Intelligence and Smart Systems (ICAIS)*, IEEE, 2021, pp. 184–89. *DOI.org (Crossref)*, https://doi.org/10.1109/ICAIS50930.2021.9395881.

[26] Barrios, et al. "Partial Discharge Classification Using Deep Learning Methods—Survey of Recent Progress." *Energies*, vol. 12, no. 13, June 2019, p. 2485. *DOI.org (Crossref)*, https://doi.org/10.3390/en12132485

[27] Florkowska, B., and M. Florkowski. "Phase-Resolved Rise-Time-Based Discrimination of Partial Discharges." *IET Generation, Transmission & Distribution*, vol. 3, no. 1, Jan. 2009, pp. 115–24. *DOI.org (Crossref)*, https://doi.org/10.1049/iet-gtd:20080171.

[28] Bodega, R., et al. "PD Recurrence in Cavities at Different Energizing Methods." *IEEE Transactions on Instrumentation and Measurement*, vol. 53, no. 2, Apr. 2004, pp. 251–58. *DOI.org (Crossref)*, https://doi.org/10.1109/TIM.2003.822478.

[29] Ahmed, N., and N. Srinivas. "PD Types and Their Detection Possibilities by PD Test Methods." *2001 Annual Report Conference on Electrical Insulation and Dielectric Phenomena (Cat. No.01CH37225)*, IEEE, 2001, pp. 307–10. *DOI.org (Crossref)*, https://doi.org/10.1109/CEIDP.2001.963545.

[30] Gutfleisch, F., and L. Niemeyer. "Measurement and Simulation of PD in Epoxy Voids." *IEEE Transactions on Dielectrics and Electrical Insulation*, vol. 2, no. 5, Oct. 1995, pp. 729–43. *DOI.org (Crossref)*, https://doi.org/10.1109/94.469970.

[31] Yii, C. C., et al. "Multi-End PD Location Algorithm Using Segmented Correlation and Trimmed Mean Data Filtering Techniques for MV Underground Cable." *IEEE Transactions on Dielectrics and Electrical Insulation*, vol. 24, no. 1, Feb. 2017, pp. 92–98. *DOI.org (Crossref)*, https://doi.org/10.1109/TDEI.2016.005902.

[32] Khan, Ammar Anwar, et al. "Investigation of Attenuation Characteristics of PD Pulse during Propagation in XLPE Cable." *2013 IEEE Power & Energy Society General Meeting*, IEEE, 2013, pp. 1–5. *DOI.org (Crossref)*, https://doi.org/10.1109/PESMG.2013.6672724.